Hindawi
Laser and Particle Beams
Volume 2022, Article ID 5671790, 6 pages
https://doi.org/10.1155/2022/5671790

Research Article

Enhancement of Magnetic Vortex Acceleration by Laser Interaction with Near-Critical Density Plasma inside a Hollow Conical Target

Xueming Li,[1] **Yue Chao**,[2] **Rui Xie**,[3] **Deji Liu**,[1] **Yuanzhi Zhou**,[2] **Shutong Zhang**,[2] **Tian Yang**,[1] **Zhanjun Liu**,[1,4] **Lihua Cao**,[1,4] **and Chunyang Zheng**[1,4]

[1]*Institute of Applied Physics and Computational Mathematics, Beijing 100094, China*
[2]*Center for Applied Physics and Technology, HEDPS, School of Physics and College of Engineering, Peking University, Beijing 100871, China*
[3]*Institute of Materials, China Academy of Engineering Physics, Jiangyou 621908, Sichuan, China*
[4]*Center for Applied Physics and Technology, HEDPS and College of Engineering, Peking University, Beijing 100871, China*

Correspondence should be addressed to Xueming Li; lixuemingst@126.com

Received 25 November 2021; Revised 16 January 2022; Accepted 26 January 2022; Published 18 February 2022

Academic Editor: Katarzyna Batani

The effects of magnetic vortex acceleration (MVA) are investigated with two-dimensional particle-in-cell (PIC) simulations by laser interaction with near-critical density (NCD) plasma inside a hollow conical plasma. Energetic and collimated proton beams can be accelerated by a longitudinal charge-separation field. Energetic protons with a peak energy of 220 MeV are produced in PIC simulations. Compared with a uniform NCD plasma, both the cutoff energy and collimation of proton beams are improved remarkably. Furthermore, the influence of different gap sizes of cone tip is taken into account. For optimizing magnetic vortex acceleration, the gap size of the cone tip is suggested to match the focal spot size of laser pulse.

1. Introduction

Ion acceleration driven by ultraintense laser pulse has huge potential advantages and a wide promising application prospect [1–3], such as proton imaging [4], hadron therapy [5], tabletop particle accelerator [6], and fast ignition of inertial confinement fusion [7, 8]. In recent years, the laser-driven high-energy ion acceleration has made much progress, and a number of researchers have explored key physical issues and techniques for obtaining high-energy ions [9–11]. At present, the acceleration mechanisms widely studied include target normal sheath acceleration (TNSA) [12, 13], radiation pressure acceleration (RPA) [14, 15], collisionless shock acceleration (CSA) [16, 17], magnetic vortex acceleration (MVA) [18–20], and so on. In these regimes, the MVA regime has an advantage in collimation, which is the potential to medical application of proton beam and beam transmission. It has been presented that the maximum ion energy can reach the GeV level with PW level laser in previous 2D and 3D computer simulations [21–23]. It is worth noting that NCD targets attracted extensive attention not only in the field of ion acceleration [24] but also in the study on brilliant gamma-ray and the generation of electron-positron pair [25].

The physical interpretation of the magnetic vortex acceleration mechanism is about the interaction between the ultraintense laser pulses and NCD plasmas. When a high-intense laser pulse propagates through a NCD target, electrons are expelled away from their initial positions, and as a result, a low-density channel is formed in the plasma. The electrons are accelerated in the direction of laser pulse propagation owing to the ponderomotive force [26]. Accordingly, the electron currents flow along the central axis and the corresponding return currents flow in the channel wall. These electron currents generate a magnetic field, circulating inside the channel around its axis. The magnetic

field appears as a form of a dipole in 2D (a toroidal vortex in 3D) moving behind the pulse. As the laser pulse exits the channel, the magnetic field quickly expands from the channel into vacuum. The magnetic pressure pushes out electrons causing a decreasing of the electron density. The charge-separation of electrons and ions forms a strong quasistatic electric field at the rear of the target, producing a collimated beam of high-energy protons.

Although there have been numerous theoretical and experimental studies of the MVA scheme, several problems remain unsolved [27, 28]. In view of that MVA scheme requires the optimal coupling condition between plasma density and length and laser power, as of yet, it has not been reported to achieve successful experiments since the parameters of plasma and laser cannot be manipulated with such precision. In those simulations, protons of MeV to GeV level energy were reached, and the required laser pulses were supposed to have hundreds of terawatts even petawatt power. It has been proposed in the previous study [28] that an enhanced magnetic vortex acceleration (EMVA) can be obtained using an advanced target where the near-critical density plasma is transversely confined between the high-Z dense wires. Such a scheme makes it possible that the magnetic vortex structure formed and the induced electrostatic field become much enhanced and stabilized.

In this study, a NCD plasma inside a conical target is introduced to improve magnetic vortex acceleration (MVA). In view of this, we utilize a hollow high-Z metal cone, which is open at both ends, to confine the near-critical plasma forming a conical target in order that the property of proton beam is able to get improvement. Two-dimensional particle-in-cell (2D PIC) simulations are carried out to investigate a laser pulse interacting with such a novel target. Simulations show the enhancement of magnetic vortex acceleration compared with a uniform NCD plasma. Both the cutoff energy and collimation of proton beams are improved remarkably.

The study is organized as follows. In Section 2, we present the simulation setup and the parameter space of 2D PIC simulations. The simulation results are presented in Section 3. The summary and conclusion are in Section 4.

2. Simulation Setup

In this study, two-dimensional simulations are carried out with PIC codes named EPOCH [29]. The size of the simulation domain is $x \times y = 100\lambda_0 \times 40\lambda_0$, and it is divided into 5000×2000 cells, where λ_0 is the vacuum laser wavelength. The grid mesh spacing is enough to resolve the minimum characteristic scale of the problem. The left boundary conditions of fields are so-called simple-laser, the top, bottom, and right conditions of fields, and the boundaries of particles are all open. A p-polarized laser pulse with wavelength of $\lambda_0 = 1.0\,\mu$m and waist $1.5\,\mu$m is incident from the left boundary of the simulation domain. It is focused to a focal spot at a distance of $6\,\mu$m from the left boundary. The laser pulse has a Gaussian spatial profile, and the pulse duration is $20T_0$, where $T_0 = 3.3\,fs$ is the laser period. The peak intensity is $2.2 \times 10^{21}\,\mathrm{W/cm^2}$, corresponding to the normalized vector potential $a_0 = 40$.

The NCD plasma target consisted of electrons and fully ionized hydrogen. Its left boundary is placed at $x = 6\,\mu$m, that is, the laser is focused at the front of the target. The length of the target between both ends is $50\lambda_0$, and the left end extends to the transverse boundaries of the simulation region. The density is $n_0 = 1.6n_c$, where $n_c = m_e\omega_0^2/4\pi e^2$ is the critical density, m_e is the electron mass, and e is the unit charge, respectively. It has been confirmed that the acceleration effectiveness has a strong dependence on the target thickness and density for a given laser power, which is based on a simple analytical model for the behavior of the EM wave inside a waveguide. Thus, the target parameters in our simulations follow the optimum condition for MVA acceleration $n_e/n_c = \sqrt{8\pi P/P_c}\,(KL_p/L_{ch})^{3/2}$ according to previous works [22, 27], where $L_p = c\tau$ is the laser pulse length, τ is the laser pulse duration, $K = 1/10$ is the geometrical factor for 2D cases, P is the laser power, $P_c = 2m_e^2c^5/e^2 = 17GW$ is the critical power for relativistic self-focusing, n_e is the electron number density, and c is the speed of light in vacuum. A hollow high-Z metal cone, which is open at both ends, is used to confine near-critical plasmas. The high-Z cone is composed of uniform aluminum plasmas with a thickness of 1.0μm, which has the same longitudinal length with the NCD plasma target. For the convenience of computation, the electron density of the high-Z cone is set to be $45n_c$. The target configuration is shown in Figure 1. The gap size of the cone tip d is equal to the diameter of the laser focal spot.

3. Simulation Results

The density profiles of proton and electron, the longitudinal electric field, the z-component of magnetic field, and the currents in x-axis direction at obvious vortex structure formation stage are presented to illustrate the MVA process. With the same setup including the laser and plasma parameters, the simulation of conventional MVA with a uniform rectangle target is performed as a comparison. The time-averaged electric field E_x and magnetic field B_z in conical target case are shown in Figures 2(a) and 2(b). The electric field and magnetic field are normalized by $m_e\omega_0c/e$ and $m_e\omega_0/e$, respectively. It is clear that the electric field and magnetic field are located at the rear side of the target in uniform rectangle target case, however, near the end of the cone in conical target case.

As shown in Figures 2(c) and 2(f), the current density along the central axis of the channel is approximately equal to the return current flowing in the walls of the channel, which can screen the magnetic field outside the channel. The electromagnetic energy is perfectly confined inside the self-generated channel, as discussed in previous studies [30]. The self-generated magnetic field plays an important role in proton acceleration by the MVA mechanism. It can be clearly seen that the growth of the electric field is related to the expansion of the magnetic field. The magnetic field pushes out electrons causing a long-living positively charged region and induces a longitudinal electric field. This

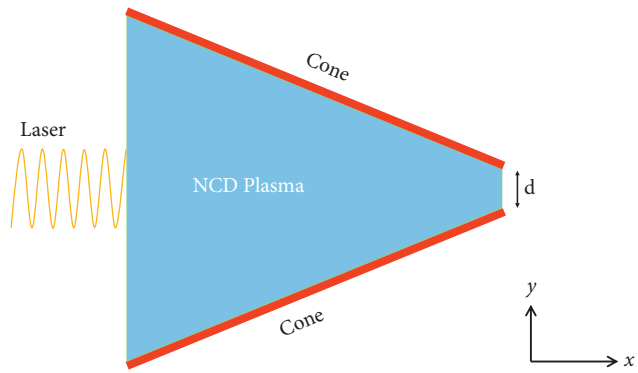

FIGURE 1: Scheme of target. The near-critical density plasma (gray) is confined in a hollow high-Z metal cone (red).

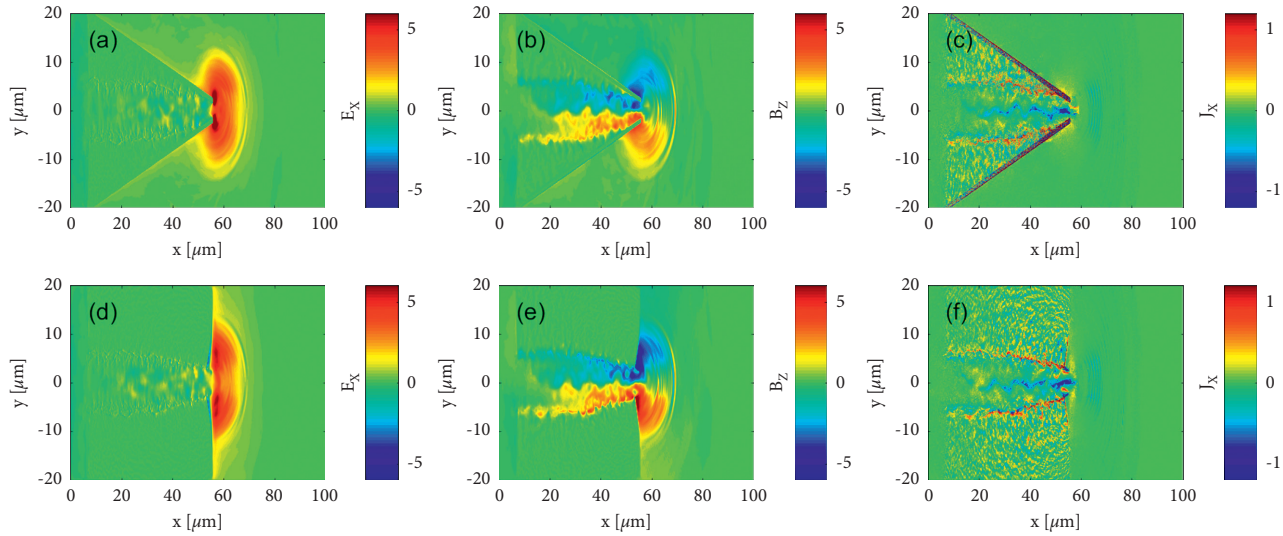

FIGURE 2: Snapshots of the time-averaged electric field E_x ((a), (d)) normalized by $m_e\omega_0 c/e$, the z-component of magnetic field B_z, ((b), (e)) normalized by $m_e\omega_0/e$ and currents in x-axis direction J_x, and ((c), (f)) normalized by ecn_c at $t = 85T_0$ for the conical target (top) and the uniform rectangle target (bottom).

structure moves together with the expanding dipole vortex. The resulting charge-separation electric field will accelerate and collimate ions from the thin filament. As mentioned in [19], the electric field moves together with the expanding magnetic dipole vortex, and the background ions located ahead of the electric field are reflected by the moving potential and gain velocity which is roughly twice the velocity of vortex. It is easy to notice the approximately similar distributions pattern between self-generated magnetic field B_z and electric field E_x. By comparison, the magnetic field in conical target is attached the cone wall, and the electric field is more concentrated. In the density profile of proton, a proton filament is produced along the laser axis behind the cone tip gap.

Figure 3 shows the electron and proton density profile of two cases at $t = 85T_0$, which are normalized by n_c. The laser pulse passes through plasma and creates a channel in both electron and ion density. There forms a thin proton filament along the central axis. The protons from the filamentation get acceleration by the longitudinal quasistatic electric field. It can be seen that the density of filament near the cone tip is higher than that in the rear of uniform rectangle target.

The snapshots of phase space of protons in the uniform rectangle target and the conical target at $t = 160T_0$ are shown in Figure 4. The phase plot of proton displays a ramp momentum distribution, which indicates that the acceleration of the proton occurs behind the target. As shown in Figure 4(a), it can be noted that the maximum proton momentum in conical target reaches $0.68m_pc$ and the corresponding proton energy is approximately 220MeV, which is consistent with the cutoff energy of the energy spectrum shown in Figure 5. The maximum proton momentum in uniform rectangle target is $0.6m_pc$ in Figure 4(b), obviously lower than that in conical target. The difference of both cases approaches about 10%.

In Figure 6, angular divergence is displayed between these two cases. The r target represents the uniform rectangle target and the c target represents the conical target. Such a narrow angular dispersion is the typical characteristic feature of MVA, which makes it possible to get a promising candidate for an ion source for hadron cancer therapy [31].

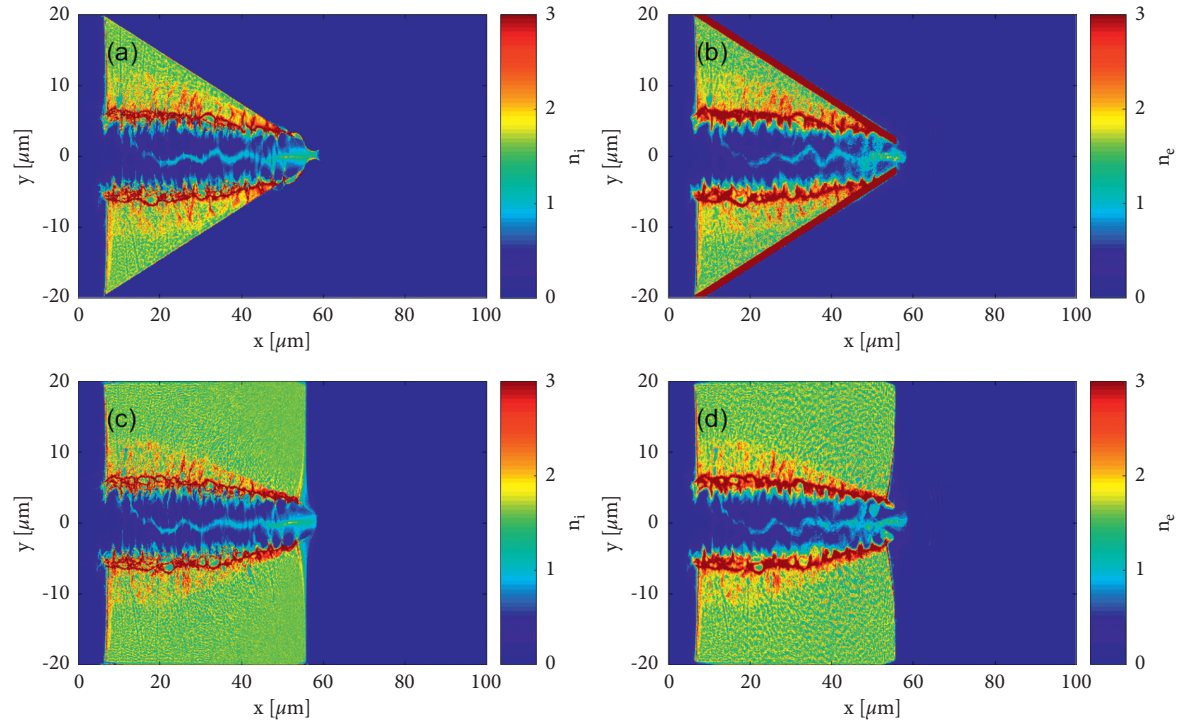

FIGURE 3: Snapshots of ion density (a) and electron density (b) for the conical target and ion density (c) and electron density (d) for the uniform rectangle target at $t = 85T_0$ MVA, which are normalized by n_c.

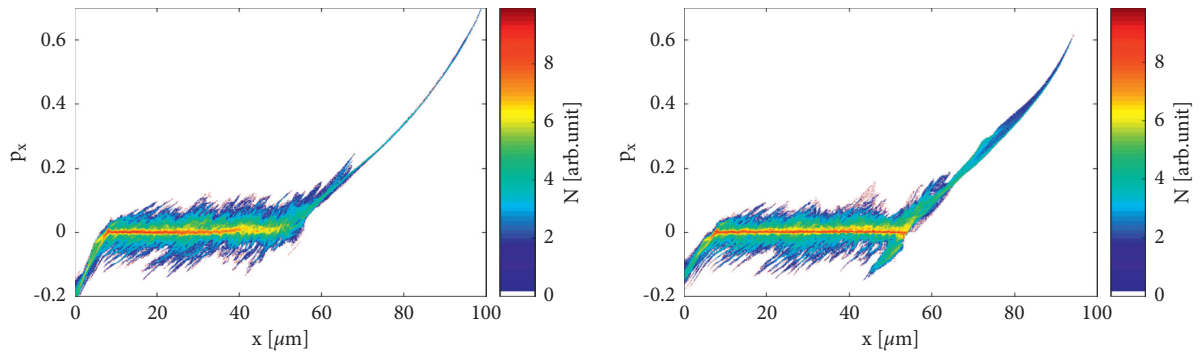

FIGURE 4: Snapshots of phase space $(p_x - x)$ of protons in the conical target (a) and the uniform rectangle target (b) at $t = 160T_0$. The momentum is normalized by $m_p c$, where m_p is the proton mass, and c is the speed of light in vacuum.

Apparently, the angular distribution of proton beams from conical target is more concentrated to the central axis. Meanwhile, the number of protons within 0.1π divergence angle in the conical target is larger than that in the uniform rectangle target. It is evident that the confinement effect of conical target helps to improve the collimation of proton beams.

Finally, in order to investigate the effect of different gap sizes of cone tip to MVA, our simulations are carried out for several cases corresponding $d = 5.0, 3.0, 2.0, 1.0, 0.5\mu$m, in which the gap size is of the order of the diameter of the laser focal spot size. The energy spectra of accelerated protons in different cases are shown in Figure 5. It can be clearly seen that the proton cutoff energy in the conical target is higher than that in the rectangle target. However, as the gap width decreases from 3.0μm to 0.5μm, the cutoff energy decreases. Obviously, smaller gap sizes of cone tip do not mean more enhanced MVA. It can be explained that small gap may make against the formation of plasmas channel, and thus, MVA would be affected. Therefore, it is suggested that gap size of cone tip prefers to be the size of the laser focal spot.

4. Summary

The effects of a NCD plasma with a conical target or a uniform rectangle target on the MVA mechanism are studied in this study. The simulations are carried out for a tightly focused high-intensity laser pulse interaction with near-critical density plasma inside a hollow conical target. The results prove that the conical guiding structure is helpful for the generation

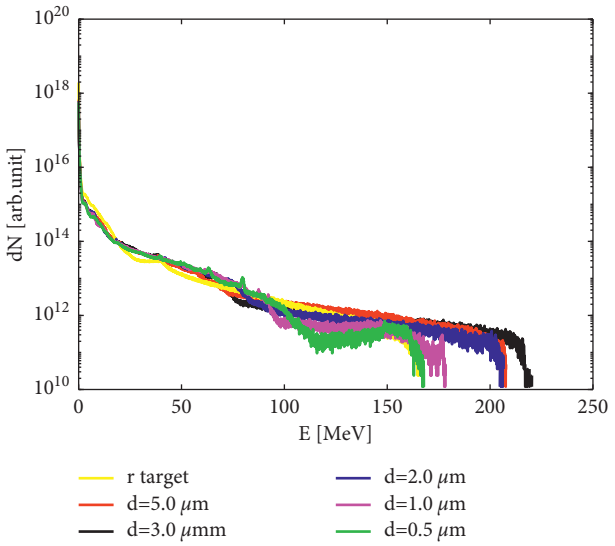

FIGURE 5: The proton energy spectra of the conical target with different gap sizes ($d = 5.0, 3.0, 2.0, 1.0, 0.5\mu$m) and the uniform rectangle targets (r target) at the final stage $t = 160T_0$.

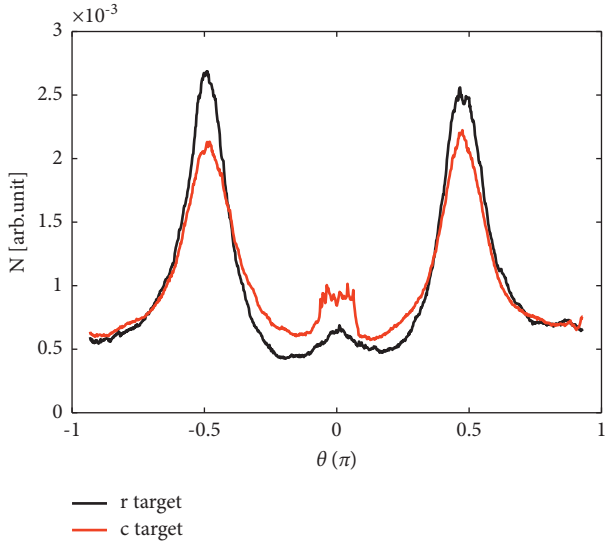

FIGURE 6: The angle distributions (with respect to the laser axis) of protons in the uniform rectangle target (r target) and the conical target (c target) at $t = 160T_0$.

of high-energy protons. For typical laser and plasma parameters, the magnetic vortex structure forms at the density gradient and induces charge-separation electric field between electrons and protons to accelerate protons to a peak energy of 220 MeV. It also shows the enhancement of magnetic vortex acceleration on the collimation and cutoff energy of proton beams. By using conical target, the near-critical density plasmas are confined in a high-Z cone. The electric field and magnetic field at the rear side of the target get more localized. As a result, the accelerated protons get more collimated and more energetic. Besides, the optimal gap size of conical target tip is supposed to match the size of the laser focal spot in order to improve MVA.

Data Availability

The data used to support the findings of this study are available from the corresponding author upon request.

Conflicts of Interest

The authors declare that they have no conflicts of interest.

Acknowledgments

This work was supported by the National Natural Science Foundation of China (11875091 and 11975059) and the Science and Technology on Plasma Physics Laboratory at CAEP (JCKYS2019212012).

References

[1] G. A. Mourou, T. Tajima, and S. V. Bulanov, "Optics in the relativistic regime," *Reviews of Modern Physics*, vol. 78, no. 2, pp. 309–371, 2006.

[2] P. Varshnety, V. Sajal, P. Chauhan, R. Kumar, and N. K. Sharma, "Effects of transverse static electric field on terahertz radiation generation by beating of two transversely modulated Gaussian laser beams in a plasma," *Laser and Particle Beams*, vol. 32, no. 3, pp. 375–381, 2014.

[3] A. Macchi, M. Borghesi, and M. Passoni, "Ion acceleration by superintense laser-plasma interaction," *Reviews of Modern Physics*, vol. 85, no. 2, pp. 751–793, 2013.

[4] M. Borghesi, A. J. Mackinnon, D. H. Campbell et al., "Multi-mev proton source investigations in ultraintense laser-foil interactions," *Physical Review Letters*, vol. 92, Article ID 055003, 2004.

[5] B. Damato, A. Kacperek, M. Chopra, I. R. Campbell, and R. D. Errington, "Proton beam radiotherapy of choroidal melanoma: the liverpool-clatterbridge experience," *International Journal of Radiation Oncology, Biology, Physics*, vol. 62, no. 5, pp. 1405–1411, 2005.

[6] M. Kaluza, J. Schreiber, M. I. Santala et al., "Influence of the laser prepulse on proton acceleration in thin-foil experiments," *Physical Review Letters*, vol. 93, Article ID 045003, 2004.

[7] D. Strickland and G. Mourou, "Compression of amplified chirped optical pulses," *Optics Communications*, vol. 56, no. 3, pp. 219–221, 1985.

[8] M. Tabak, J. Hammer, M. E. Glinsky et al., "Ignition and high gain with ultrapowerful lasers," *Physics of Plasmas*, vol. 1, no. 5, pp. 1626–1634, 1994.

[9] H. Daido, M. Nishiuchi, and A. S. Pirozhkov, "Review of laser-driven ion sources and their applications," *Reports on Progress in Physics*, vol. 75, no. 5, Article ID 056401, 2012.

[10] D. Calestani, M. Villani, G. Cristoforetti et al., "Fabrication of zno-nanowire-coated thin-foil targets for ultra-high intensity laser interaction experiments," *Matter and Radiation at Extremes*, vol. 6, no. 4, Article ID 046903, 2021.

[11] Y. Chao, X. Yan, R. Xie et al., "Enhanced proton acceleration by laser-driven collisionless shock in the near-critical density target embedding with solid nanolayers," *Laser and Particle Beams*, vol. 2021, Article ID 7047548, 2021.

[12] S. C. Wilks, A. B. Langdon, T. E. Cowan et al., "Energetic proton generation in ultra-intense laser-solid interactions," *Physics of Plasmas*, vol. 8, no. 2, pp. 542–549, 2001.

[13] P. Mora, "Plasma expansion into a vacuum," *Physical Review Letters*, vol. 90, no. 18, Article ID 185002, 2003.
[14] X. Q. Yan, C. Lin, Z. M. Sheng et al., "Generating high-current monoenergetic proton beams by a CircularlyPolarized laser pulse in the phase-StableAcceleration regime," *Physical Review Letters*, vol. 100, no. 13, Article ID 135003, 2008.
[15] A. P. L. Robinson, M. Zepf, S. Kar, R. G. Evans, and C. Bellei, "Radiation pressure acceleration of thin foils with circularly polarized laser pulses," *New Journal of Physics*, vol. 10, no. 1, Article ID 013021, 2008.
[16] S. Tochitsky, A. Pak, F. Fiuza et al., "Laser-driven collisionless shock acceleration of ions from near-critical plasmas," *Physics of Plasmas*, vol. 27, no. 8, Article ID 083102, 2020.
[17] R. Xie, L. H. Cao, J. X. Gong et al., "Improvement of proton acceleration via collisionless shock acceleration by laser-foil interaction with an external magnetic field," *Physics of Plasmas*, vol. 26, no. 12, Article ID 123102, 2019.
[18] S. V. Bulanov, T. Z. Esirkepov, F. Califano et al., "Generation of collimated beams of relativistic ions in laser-plasma interactions," *Journal of Experimental and Theoretical Physics Letters*, vol. 71, no. 10, pp. 407–411, 2000.
[19] T. Nakamura, S. V. Bulanov, T. Z. Esirkepov, and M. Kando, "High-energy ions from near-critical density plasmas via magnetic vortex acceleration," *Physical Review Letters*, vol. 105, no. 13, Article ID 135002, 2010.
[20] Y. Fukuda, A. Y. Faenov, M. Tampo et al., "Energy increase in multi-mev ion acceleration in the interaction of a short pulse laser with a cluster-gas target," *Physical Review Letters*, vol. 103, no. 16, Article ID 165002, 2009.
[21] A. Sharma and A. Andreev, "Effective laser driven proton acceleration from near critical density hydrogen plasma," *Laser and Particle Beams*, vol. 34, no. 2, pp. 219–229, 2016.
[22] S. S. Bulanov, V. Y. Bychenkov, V. Chvykov et al., "Generation of gev protons from 1 pw laser interaction with near critical density targets," *Physics of Plasmas*, vol. 17, no. 4, Article ID 043105, 2010.
[23] A. Sharma, "High energy electron and proton acceleration by circularly polarized laser pulse from near critical density hydrogen gas target," *Scientific Reports*, vol. 8, no. 1, p. 2191, 2018.
[24] J. H. Bin, W. J. Ma, H. Y. Wang et al., "Ion acceleration using relativistic pulse shaping in near-critical-density plasmas," *Physical Review Letters*, vol. 115, Article ID 064801, 2015.
[25] X.-L. Zhu, M. Chen, T.-P. Yu, S.-M. Weng, F. He, and Z.-M. Sheng, "Collimated GeV attosecond electron-positron bunches from a plasma channel driven by 10 PW lasers," *Matter and Radiation at Extremes*, vol. 4, no. 1, Article ID 014401, 2019.
[26] S. V. Bulanov, D. V. Dylov, T. Z. Esirkepov, F. F. Kamenets, and D. V. Sokolov, "Ion acceleration in a dipole vortex in a laser plasma corona," *Plasma Physics Reports*, vol. 31, no. 5, pp. 369–381, 2005.
[27] N. Zhao, J. Jiao, D. Xie et al., "Near-100 mev proton acceleration from 1021 W/cm2 laser interacting with near-critical density plasma," *High Energy Density Physics*, vol. 37, Article ID 100889, 2020.
[28] W. L. Zhang, B. Qiao, X. F. Shen et al., "Monoenergetic ion beam acceleration from transversely confined near-critical plasmas by intense laser pulses," *Physics of Plasmas*, vol. 24, no. 9, Article ID 093108, 2017.
[29] T. D. Arber, K. Bennett, C. S. Brady et al., "Contemporary particle-in-cell approach to laser-plasma modelling," *Plasma Physics and Controlled Fusion*, vol. 57, no. 11, Article ID 113001, 2015.
[30] J. Park, S. S. Bulanov, J. Bin et al., "Ion acceleration in laser generated megatesla magnetic vortex," *Physics of Plasmas*, vol. 26, no. 10, Article ID 103108, 2019.
[31] S. S. Bulanov, E. Esarey, C. B. Schroeder et al., "Helium-3 and helium-4 acceleration by high power laser pulses for hadron therapy," *Physical Review Accelerators and Beams*, vol. 18, Article ID 061302, 2015.